Transcytosis of IgA Attenuates *Salmonella* Invasion in Human Enteroids and Intestinal Organoids

Cait M. Costello,[a] Graham G. Willsey,[b] Angelene F. Richards,[b] Jaeyoon Kim,[a] Matteo S. Pizzuto,[c] Stefano Jaconi,[c] Fabio Benigni,[c] Davide Corti,[c] [ID]Nicholas J. Mantis,[b] [ID]John C. March[a]

[a]Department of Biological and Environmental Engineering, Cornell University, Ithaca, New York, USA
[b]Division of Infectious Diseases, Wadsworth Center, New York State Department of Health, Albany, New York, USA
[c]Humabs BioMed SA a Subsidiary of Vir Biotechnology Inc., Bellinzona, Switzerland

ABSTRACT Secretory IgA (SIgA) is the most abundant antibody type in intestinal secretions where it contributes to safeguarding the epithelium from invasive pathogens like the Gram-negative bacterium, *Salmonella enterica* serovar Typhimurium (STm). For example, we recently reported that passive oral administration of the recombinant monoclonal SIgA antibody, Sal4, to mice promotes STm agglutination in the intestinal lumen and restricts bacterial invasion of Peyer's patch tissues. In this report, we sought to recapitulate Sal4-mediated protection against STm in human Enteroids and human intestinal organoids (HIOs) as models to decipher the molecular mechanisms by which antibodies function in mucosal immunity in the human gastrointestinal tract. We confirm that Enteroids and HIO-derived monolayers are permissive to STm infection, dependent on HilD, the master transcriptional regulator of the SPI-I type three secretion system (T3SS). Stimulation of M-like cells in both Enteroids and HIOs by the addition of RANKL further enhanced STm invasion. The apical addition of Sal4 mouse IgA, as well as recombinant human Sal4 dimeric IgA (dIgA) and SIgA resulted a dose-dependent reduction in bacterial invasion. Moreover, basolateral application of Sal4 dIgA to Enteroid and HIO monolayers gave rise to SIgA in the apical compartment via a pathway dependent on expression of the polymeric immunoglobulin receptor (pIgR). The resulting Sal4 SIgA was sufficient to reduce STm invasion of Enteroid and HIO epithelial cell monolayers by ~20-fold. Recombinant Sal4 IgG was also transported in the Enteroid and HIOs, but to a lesser degree and via a pathway dependent on the neonatal Fc receptor (FCGRT). The models described lay the foundation for future studies into detailed mechanisms of IgA and IgG protection against STm and other pathogens.

KEYWORDS FCRN, PIGR, SAL4, *Salmonella*, enteroids, monoclonal antibodies, organoids

The Centers for Disease Control and Prevention (CDC) estimates that *Salmonella* cause in excess of 1.35 million infections and more than 25,000 hospitalizations in the United States every year. Globally, the bacterium is a leading cause of diarrheal disease in children and adults, as well as the etiologic agent of typhoid fever. With the emergence of multidrug resistant strains of typhoidal and nontyphoidal *Salmonella* in virtually every corner of the world, there is mounting pressure to develop alternatives to antibiotics in the prevention and control of disease. The capacity of *Salmonella* to breach the intestinal epithelial barrier is a pivotal event in the infection process, leading to local inflammation, gastroenteritis, and in some instances, bacteremia and systemic infection (1). Arguably, the most well-studied *Salmonella* serovar is *Salmonella enterica* serovar Typhimurium (STm). The bacterium employs flagella-based motility and a multitude of adhesins (e.g., fimbriae, pili) to secure contact with the apical surfaces of intestinal epithelial cells (IECs). From there, STm gains entry into IECs using a
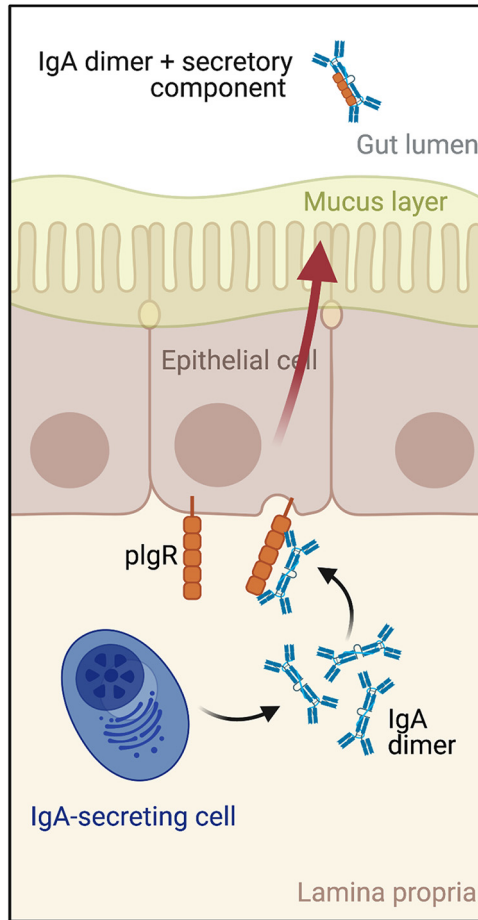
FIG 1 Schematic representation of IgA transcytosis and secretory IgA (SIgA) formation. SIgA is delivered into intestinal secretions through a process involving intestinal epithelial cells themselves. Specifically, B cells located in the gut mucosa secrete dimeric IgA (dIgA), which is recognized by the polymeric immunoglobulin receptor (pIgR) on the basolateral surfaces of intestinal epithelial cells. The pIgR transports dIgA from basolateral to apical cell surfaces, where dIgA is then released into the intestinal lumen in complex with secretory component (SC), an ~70 kDa proteolytic fragment of pIgR. Thus, in its final form, SIgA is an assemblage of two IgA monomers and SC.

specialized *Salmonella* pathogenicity island-1 (SPI-1) encoded type-three secretion system (T3SS-1) that is transcriptionally controlled by HilD, along with an array of effector proteins involved in actin depolymerization and membrane remodeling (2). The bacterium can survive intracellularly within *Salmonella*-containing vacuoles (SCVs) or exit epithelial cells and take up residence in dendritic cells and/or macrophages located in the intestinal mucosa. When administered intragastrically to mice, STm preferentially invade M cells, a specialized epithelial cell type located overlying gut-associated lymphoid tissues such as Peyer's patches (3–6).

A fundamental feature of the human immune response to enteric pathogens like STm is the production of vast quantities of secretory IgA (SIgA) antibodies. SIgA is the most abundant class of antibody in intestinal secretions, where concentrations can exceed 1000 μg/mL (7). SIgA is delivered into the intestinal lumen via active transport across the epithelial barrier (Fig. 1). Specifically, B cells located in the gut mucosa secrete dimeric IgA (dIgA), which is recognized by the polymeric immunoglobulin receptor (pIgR) and transported from the basolateral to apical epithelial cell surface via transcytosis. The dIgA is then released into the intestinal lumen in complex with secretory component (SC), an ~70 kDa proteolytic fragment of pIgR (8). Thus, in its final form, SIgA is an assemblage of two IgA monomers and SC (9, 10). Once released into the intestinal lumen, SIgA protects the intestinal epithelium from pathogens through a

process known as "immune exclusion" via antigen and pathogen cross-linking, entrapment in the intestinal mucus, and eventual clearance from the gastrointestinal tract through peristalsis (11).

Sal4 is a well-characterized IgA monoclonal antibody (MAb) isolated from mice immunized with an attenuated strain of STm (12). Sal4 recognizes the O5-antigen of STm lipopolysaccharide (LPS) (13) and has been shown to block STm invasion into HeLa cells *in vitro* (5, 6). In the so-called backpack tumor model, it was shown that Sal4 IgA, when actively transported into the intestinal lumen of mice in form of secretory IgA (SIgA), was able to reduce STm uptake into Peyer's patch tissues (13). Peyer's patch M cells represent the point of entry for invasive strains of *Salmonella enterica* and the bottleneck for systemic dissemination (14). Recently, we produced and characterized recombinant human SIgA versions of Sal4. We demonstrated by flow cytometry, light microscopy, and fluorescence microscopy that Sal4 SIgA promotes the formation of large, densely packed bacterial aggregates *in vitro*. Using a mouse model, we also showed that oral administration of Sal4 SIgA entrapped STm within the intestinal lumen and reduced bacterial invasion into gut-associated lymphoid tissues by several orders of magnitude (5). In addition to promoting bacterial agglutination, Sal4 IgA is also a potent inhibitor of STm flagella-based motility and SPI-1 mediated invasion of epithelial cells *in vivo* (15). Sal4 IgA also impacts STm transit time and shedding in the gut (16), although the exact mechanisms by which Sal4 IgA prevents bacterial uptake into Peyer's patch tissues have not been fully resolved.

While most studies with SIgA have been conducted using *in vitro* approaches and *in vivo* mouse models, SIgA function in the context of the human intestine has remained largely unknown. Human Enteroids and human intestinal organoids (HIOs) have revolutionized our ability to probe the molecular interactions between the human intestinal mucosa and invasive bacterial pathogens like STm (17–20). There are many similarities between HIOs and Enteroids; however, HIOs are fetal-like and are generated from the directed differentiation of pluripotent stem cells (21), whereas Enteroids are generated from crypt fractions from intestinal tissue explants and typically represent mature adult tissue (22). These cells have the potential to self-organize into intestinal tissue-like structures that contain a high percentage of nonenterocyte cell types, including Goblet cells and enteroendocrine cells and M-like cells. It is now possible to use Enteroids and HIOs to investigate how different intestinal epithelial cell types (e.g., M cells), physical forces (e.g., shear stress), and stress-activated signaling pathways (e.g., TLR4, NF-κB) influence infection and inflammation (23–25). Others have used Enteroids and HIOs to study STm pathogenesis in detail (26–28).

In their three-dimensional state, the apical membrane of Enteroids and HIOs is only accessible to bacteria and xenobiotics by microinjection (26, 29, 30). In order to use Enteroids and HIOs to study transcytosis, access to both the apical and basal epithelial membranes is required. Protocols now exist for the culture of Enteroids as 2-D monolayers on Transwell inserts and scaffolds (17, 31–34) which allow easy access to both the apical and basolateral membranes. Enteroids are typically cultured in high wnt media, allowing formation of 2-D monolayers from a 3-D cyst due to the high numbers of proliferating undifferentiated cells. We and others have found that supplementing media with exogenous wnt agonist (Chir99021) and Rock Inhibitor also enables pluripotent-stem cell derived HIOs to be cultured on Transwells (35–37).

In this report, we sought to recapitulate Sal4-mediated protection against STm in Enteroids and HIOs to show that these models can be used to decipher the molecular mechanisms by which antibodies function in mucosal immunity in human gastrointestinal tract. We observed that the induction of M-like cells in Enteroids and HIO-derived monolayers significantly enhanced STm invasion in a SPI-1 dependent manner. Moreover, our studies showed for the first time that IgA transcytosis can occur in a human organoid model. We showed that basolateral application of Sal4 dIgA to Enteroid and HIO monolayers enabled transcytosis to the apical compartment via a pathway dependent on expression of the polymeric immunoglobulin receptor (pIgR).

The resulting Sal4 SIgA was sufficient to reduce STm invasion of Enteroid and HIO epithelial cell monolayers by ~20-fold. Recombinant Sal4 IgG was also transported in the Enteroid and HIOs, but to a lesser degree and via a pathway dependent on the neonatal Fc receptor (FCGRT). These findings reveal the potential of both Enteroid and HIO monolayer models to study IgA and IgG transcytosis and protection against infection.

RESULTS

RANKL induces M-like cell formation in both Enteroid and HIO monolayers leading to increased and localized STm invasion. It has been reported that M-like cells are induced in Enteroid and HIOs by the addition of RANKL (38–40). To confirm this in our model, Enteroid and HIO monolayers were prepared as described in Materials and Methods and treated with RANKL for 5 days. M-like cells were then visualized within HIO and Enteroid monolayers via confocal microscopy and immunofluorescence staining with anti-GP2 (Fig. 2A and B). After 7 days, mRNA expression of M-like cell markers SpiB and GP2 were assessed via qRT-PCR. Transcription of both genes significantly increased in RANKL-treated monolayers relative to untreated control monolayers (Fig. 2C–D), while mRNA levels of RANK, the receptor for RANKL, were not affected (Fig. 2E). HIOs appeared to express more M-like cells than Enteroids following RANKL treatment, as evidenced by the increase in staining for GP2 in HIOs and increase in M cell marker transcript abundance. To assess the impact of RANKL-treatment on STm invasion, RANKL-treated and untreated control Enteroid and HIO monolayers were inoculated with STm 14028s for 2 h, after which intracellular bacteria were quantified through gentamicin protection assay. STm invasion increased significantly in RANKL-treated Enteroids and HIOs, compared to non-RANKL treated controls (Fig. 2F). Moreover, HIOs were more susceptible to invasion than Enteroids, which correlates with the increased number of M-like cells in HIO compared to Enteroids. STm invasion was further shown to be dependent on the SPI-1 type 3 secretion system (T3SS-1) (Fig. 3). Confocal imaging revealed that GFP-tagged STm WT localized inside the HIOs, while STm Δ*hilD* was largely excluded from the epithelial layer. These observations were further confirmed through gentamicin invasion assays, which revealed the *hilD* deletion strain exhibited ~1000-fold decrease in invasion relative to WT STm (Fig. 3).

Apically administered Sal4 IgA and Sal4 IgG significantly reduces STm invasion of M cells in Enteroid and HIO monolayers. Sal4 IgA is an anti-LPS IgA monoclonal antibody that blocks STm invasion into HeLa cells *in vitro*, and prevents Peyer's patch infection in mice (5, 6). To investigate the ability of Sal4 IgA to protect against STm invasion of Enteroid and HIO monolayers, we employed a competitive infection assay using STm WT and two mutants, STm Δ*hilD* (T3SS-1 invasion deficient) and STm Δ*oafA* (which lacks the Sal4 epitope O5 antigen but otherwise invasion competent). Enteroid and HIO monolayers were first pretreated with either monomeric Sal4 IgA (mIgA), dimeric Sal4 IgA (dIgA), Sal4 IgG, or PBS, and then inoculated with 1:1 mixtures of STm WT and STm Δ*hilD*, or STm WT and STm Δ*oafA*. After 2 h, intracellular bacteria were enumerated via gentamicin protection assays as described above. As expected, STm Δ*hilD* had significantly reduced invasion in both Enteroid and HIO monolayers compared to both STm WT and STm Δ*oafA* (CFU/mL values of <20 CFU/mL), (Fig. 4A and B). Furthermore, the *oafA* deletion mutant did not exhibit an invasion defect relative to STm WT, confirming that the lack of the O5 antigen does not alter STm infectivity in Enteroids and HIOs. In contrast, treatment with all three Sal4 derivatives significantly inhibited STm WT invasion into both Enteroid and HIO monolayers. In line with previous reports, Sal4 mIgA and IgG were less effective than the dIgA in preventing STm invasion (6). In Enteroids, dIgA reduced WT STm invasion by 10-fold, compared to mIgA and IgG which both reduced WT STm invasion by approximately 3-fold. However, the trend proved not to be statistically significant. Similarly, in HIOs dIgA was more effective than mIgA and IgG in reducing STM invasion (4.5-fold compared to 3-fold and 2.5-fold, respectively). Again, the difference did not achieve statistical significance. In contrast, none of the three Sal4 MAbs affected STm Δ*oafA* invasion.

Transcytosis of Sal4 IgA and Sal4 IgG can occur in Enteroid and HIO monolayers. We next sought to examine whether Sal4 IgA transcytosis could be recapitulated in either the HIO or Enteroid models. Transcytosis is mediated by pIgR *in vivo*. In preliminary
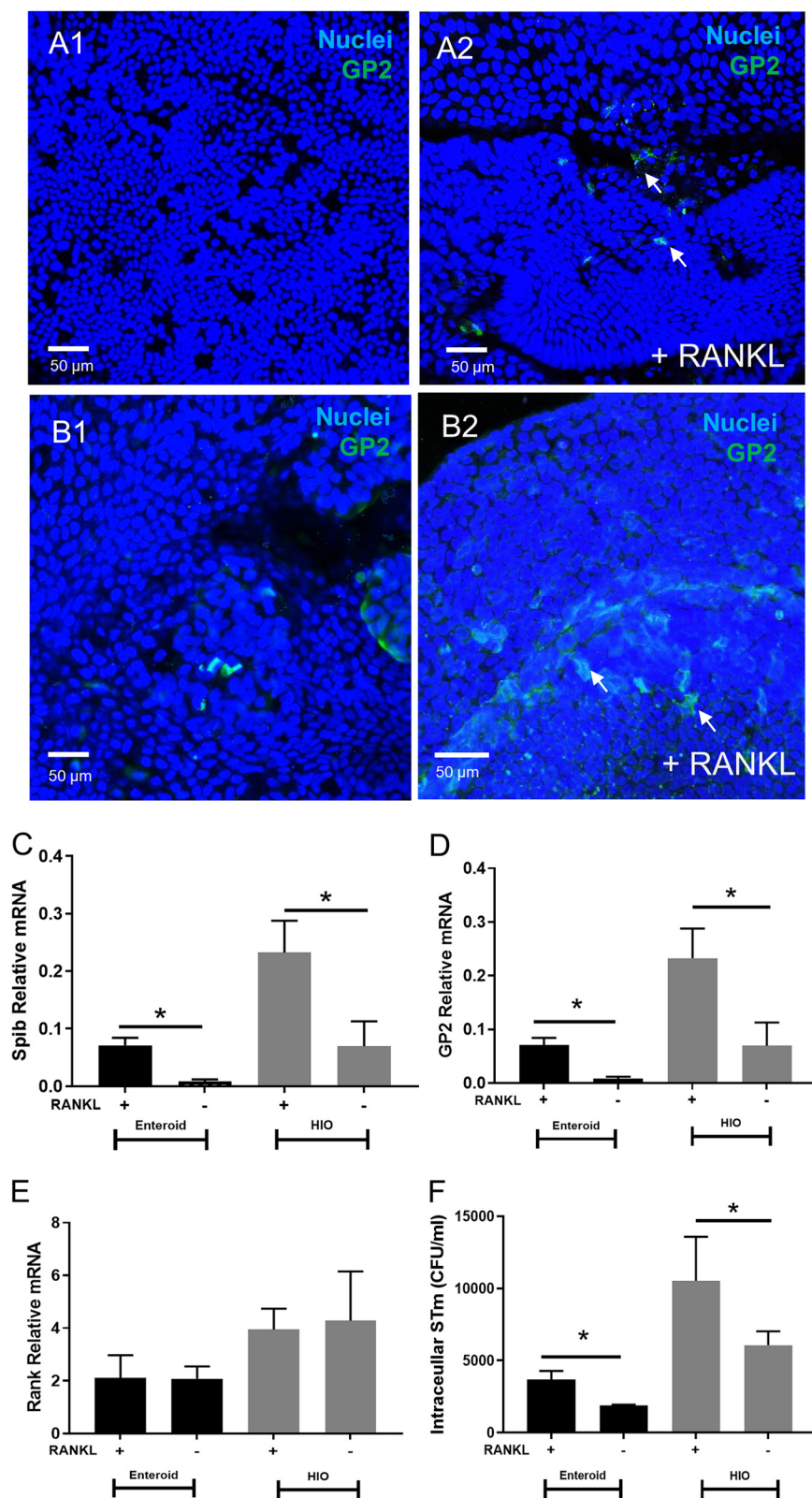
FIG 2 Induction of M Cell formation in Enteroids and HIOs Enhances STm Invasion. Addition of RANKL (100 ng/mL) enriches M cells, as determined by GP2 staining in Enteroids (A) and HIOs (B). RANKL significantly increases GP2 and Spi-B mRNA (C, D) but not RANK receptor (E). WT STm (0.01 OD$_{600}$) was applied for 2 h to monolayers treated with and without RANKL. Results show RANKL treated monolayers have significantly increased STm invasion in a gentamicin invasion assay (F) *, $P < 0.05$, one-way ANOVA with Tukey posttest. Confocal images shown are representative images from ($n = 3$) biological replicates.
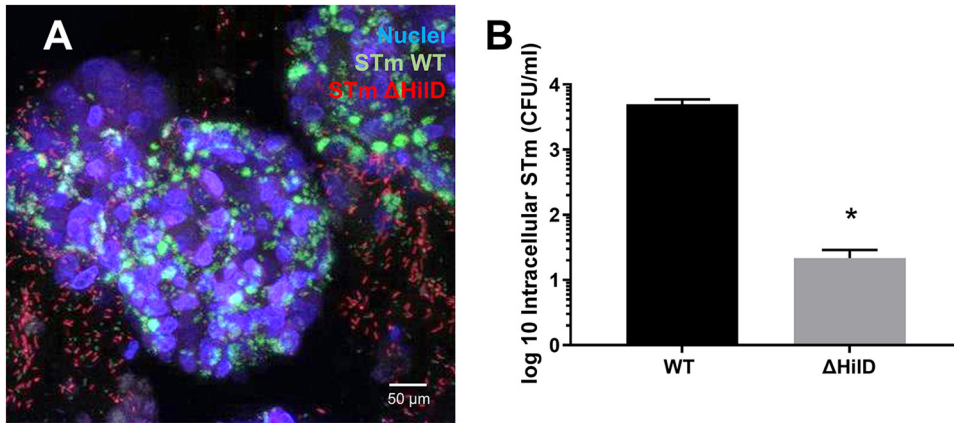
FIG 3 STm invasion into HIO Monolayers is Dependent on SPI-1 T3SS. HIOs were infected for 2 h with WT STm and $\Delta hilD$ (0.01 OD_{600}). Confocal images (A) show that WT STm (green) is able to permeate the epithelial layer and invade the organoid, but not $\Delta hilD$ (red) which is mostly excluded from the epithelial layer. Using a gentamicin invasion assay (B) we show that HilD has significantly reduced invasion into HIOs by (1000-fold). *, $P < 0.05$, one-way ANOVA with Tukey post test. Invasion assays are combined data from ($n = 3$) biological replicates.

experiments we found that HIOs express low levels of pIgR, but expression could be induced through IL-1 or IFNγ treatment (Fig. S1). However, IFNγ is detrimental to tight junction integrity as shown by Lucifer Yellow permeability (Fig. S2), which could lead to paracellular MAb diffusion. Therefore, HIO and Enteroid monolayers were treated with IL-1. Following a 16 h treatment with IL-1 (10 ng/mL), we assessed pIgR and FCGRT transcript abundance through qRT-PCR and protein expression via IF. pIgR staining increased following induction with IL-1 in both Enteroids and HIOs (Fig. 5A). Similarly, qRT-PCR revealed that pIgR mRNA transcript abundance increased ~20-fold in both Enteroid and HIO monolayers in response to IL-1. However, baseline pIgR expression levels differed substantially between Enteroids and HIOs prior to IL-1 stimulation (Fig. 5C).

It has been reported that IgG is also transported across polarized intestinal epithelial cells by the neonatal Fc receptor (FCGRT or FcRN). Indeed, IF (Fig. 5B) and qRT-PCR (Fig. 5D) revealed that both Enteroids and HIOs express FCGRT, although IL-1 treatment did not have a significant impact on expression. Here, HIOs expressed almost
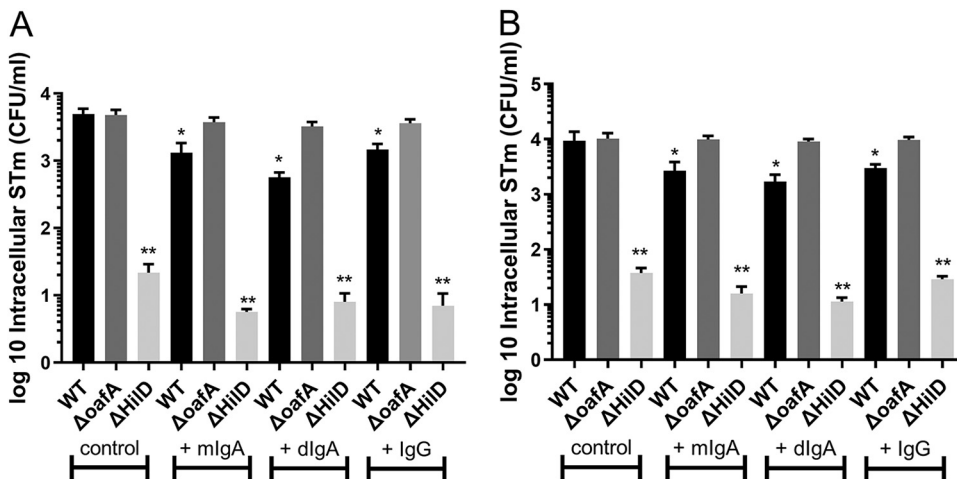

FIG 4 Apically Administered Sal4 Inhibits STm Invasion in Enteroid and HIO Monolayers. Monolayers of Enteroids and HIOs were infected for 2 h with 50 μL 0.1 OD_{600} OSTm WT or STm $\Delta oafA$ (final concentration 0.01 OD_{600}). Additional treatments were either 1 μg/mL Sal4 mIgA, Sal4 dIgA or Sal4 IgG or no antibody. STm invasion was measured through gentamicin invasion assay. Results show all antibodies significantly reduced invasion of WT STm, but not STm $\Delta oafA$ (Fig. 3A and B). *, $P < 0.05$, one-way ANOVA with Tukey post test. Invasion assays are combined data from ($n = 3$) biological replicates.
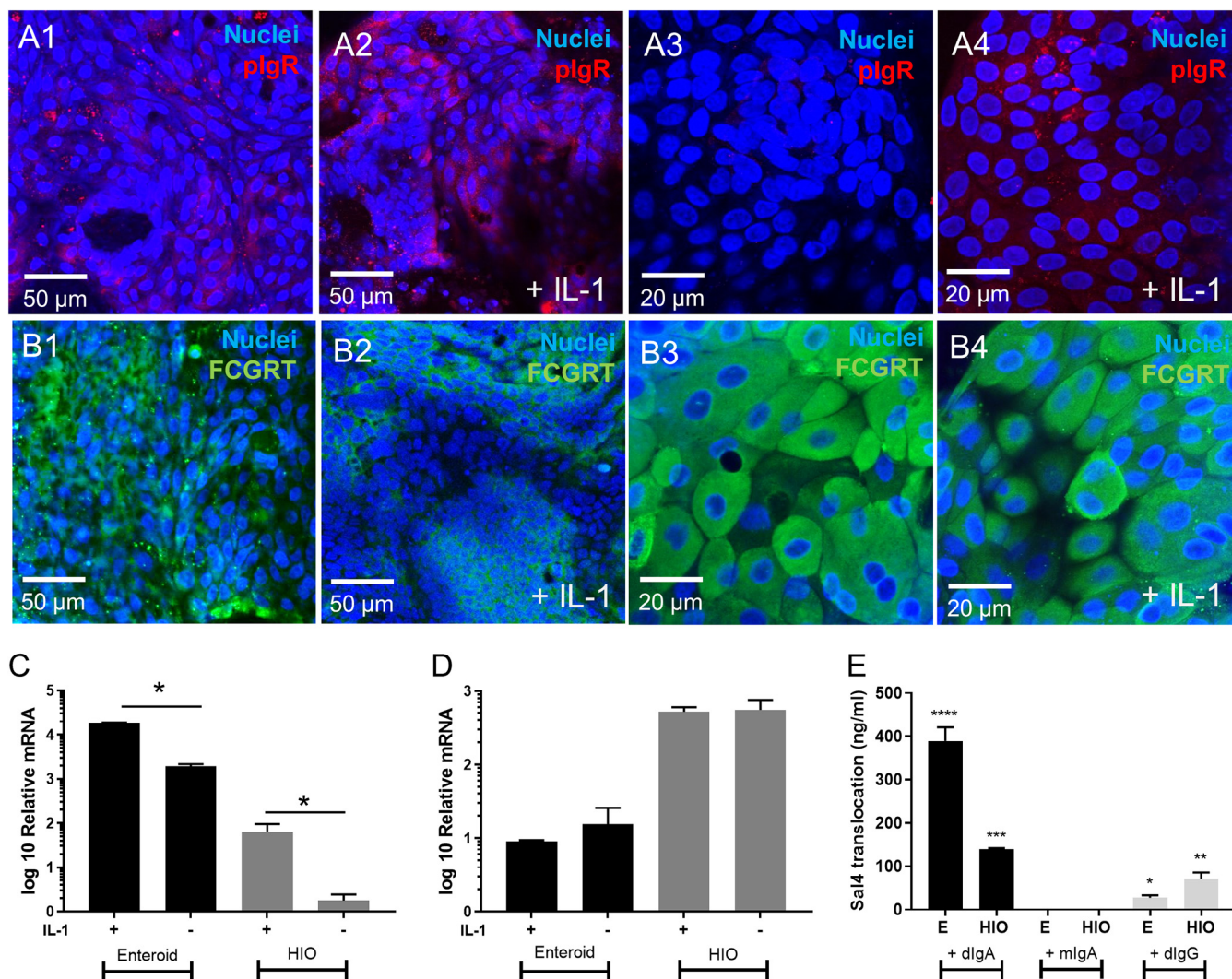
FIG 5 Expression of pIgR and FCGRT in Enteroids and Organoids for Sal4 transcytosis. Effect of IL-1 on pIgR (A) and FCGRT (B) expression in Enteroids and HIOs. Treatments shown are no IL-1 and 10 ng/mL IL-1. Confocal microscopy shows IL-1 significantly increases pIgR staining relative to control in both Enteroids and HIOs, but IL-1 does not have an effect on FCGRT expression. The effect of IL-1 was also determined by measuring relative mRNA levels of pIgR (C) and FCGRT (D). Results show IL-1 significantly increases pIgR relative to control in both Enteroids and HIOs, but IL-1 does not have an effect on FCGRT expression. Transcytosis of IgA and IgG was quantified with an ELISA using STm LPS (E). MAbs (10 μg/mL Sal4 dIgA, Sal4 mIgA and Sal4 IgG) were added to monolayers basolaterally for 16 h. Apical medium was collected for ELISA. Results show dIgA and IgG was transported through the membrane, but the monomers were not. The bar graphs depict combined data from biological replicates ($n = 3$) $P < 0.05$, one-way ANOVA with Tukey post test.

two times more FCGRT mRNA compared to Enteroids. We also examined the expression levels of other IgG receptors, including FcγR2A, FcγR2B, FcγR2C, FcγR3A and FcγR3B; however, their transcripts were not detected by qRT-PCR (data not shown). To test whether transcytosis of Sal4 occurs in across monolayers, we basolaterally administered 10 μg/mL of dIgA, mIgA, or IgG for 16 h and then assessed antibody levels in the apical compartment by ELISA. Sal4 dIgA was detected in media collected from the apical compartments of both HIO and Enteroid monolayers, while Sal4 mIgA was not detected, suggesting MAb transport was pIgR mediated (Fig. 5E). In Enteroids, ~4% of the basolateral concentration of dIgA was detected in the apical compartments, compared to just 1% in HIOs.

We also observed transport of Sal4 IgG in our Enteroid and HIO model, which suggests the existence of an IgG-specific pathway in these two monolayers (41). In Enteroids, ~0.2% of the basolateral concentration of IgG was detected in the apical compartments, compared to 0.5% in HIOs. This difference between the two cell types was statistically significant.
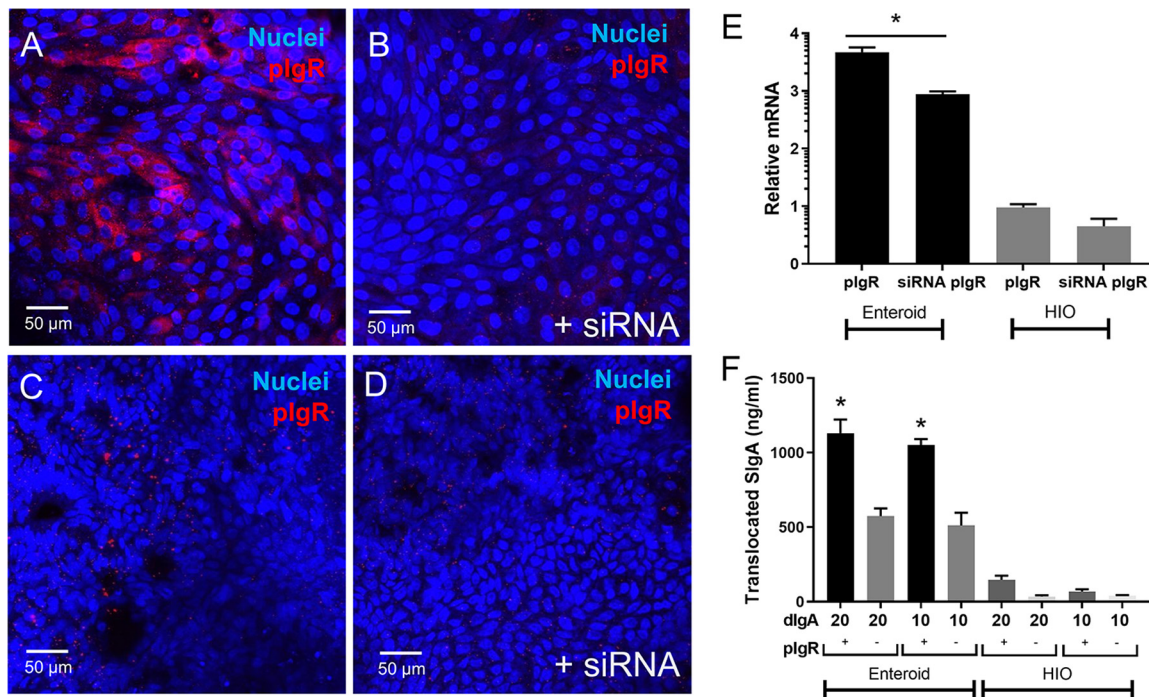
FIG 6 Secretory IgA is formed using pIgR after basolateral addition of dimeric Sal4 IgA. Monolayers were incubated with siRNA to knockdown pIgR expression. Results are confocal imaging of Enteroid monolayers (A–B) and HIO monolayers (C–D) stained for pIgR (red) and nuclei (blue) after incubation for 36 h with siRNA. Images shown are representative images from ($n = 3$) technical replicates from ($n = 2$) biological experimental replicates. Results show pIgR staining decreases in intensity with addition siRNA. Knockdown was further confirmed with qPCR (E). Results show relative mRNA levels of pIgR is significantly reduced with siRNA in Enteroids but not HIOs. Antibodies (10 and 20 μg/mL Sal4 dIgA) were added to monolayers basolaterally for 16 h. Apical medium was collected for a sIgA ELISA. Results show both 10 and 20 μg/mL Sal4 dIgA results in significantly more SIgA formation in control Enteroid monolayers relative to pIgR knockdowns, but not in HIOs. Confocal images shown are representative images from ($n = 3$) biological replicates. Bar graph depict combined data from biological replicates ($n = 3$) $P < 0.05$, one-way ANOVA with Tukey post test.

Dimeric IgA is converted to secretory IgA during transcytosis in both Enteroid and HIO monolayers. Following transcytosis, a 70 kDA fragment of the pIgR known as SC remains covalently associated with dIgA, giving rise to SIgA in the intestinal lumen. The observation that Sal4 dIgA is transported across HE and HIOs prompted us to examine whether apically localized Sal4 dIgA was in fact dependent on pIgR and associated with SC. We therefore repeated the transcytosis experiment using Enteroid and HIO monolayers that were depleted of pIgR through RNAi. Confocal microscopy (Fig. 6A to D) and qRT-PCR (Fig. 6E) revealed that siRNA treatment resulted in an ~50% reduction of pIgR expression in both Enteroid and HIO monolayers.

To SC levels following basolateral administration of dIgA (20 and 10 μg/mL), we collected apical media and quantified SIgA using an SC-specific via ELISA (Fig. 6F). In Enteroids, SIgA was detected apically when 20 or 10 μg/mL dIgA was applied basolaterally. In each case, 1.1 – 1.2 μg/mL was detected apically, which corresponds to ~5–10% of the number of antibodies initially seeded in the basolateral compartment. Significantly less SC was detected in the apical compartment of siRNA-treated monolayers designed to knockdown pIgR, suggesting that the SIgA conversion is pIgR-dependent. SIgA was also detected apically in HIO monolayers (Fig. 6F), however at a much lower concentration than Enteroids, with 0.5–1% of the basolateral concentration detected. There was no significant difference to the siRNA knockdown in HIOs, potentially due to the lower native levels of pIgR shown in Fig. 5A.

Basolateral application of Sal4 to Enteroid and HIO monolayers protects M cells against STm invasion. Finally, we sought to examine whether basolateral application of Sal4 IgA (and IgG) can reduce apically mediated STm invasion of Enteroid and HIO monolayers. To test this, Enteroid and HIO monolayers were treated basolaterally with Sal4 mIgA, dIgA, or IgG, and then incubated overnight to allow transcytosis. The
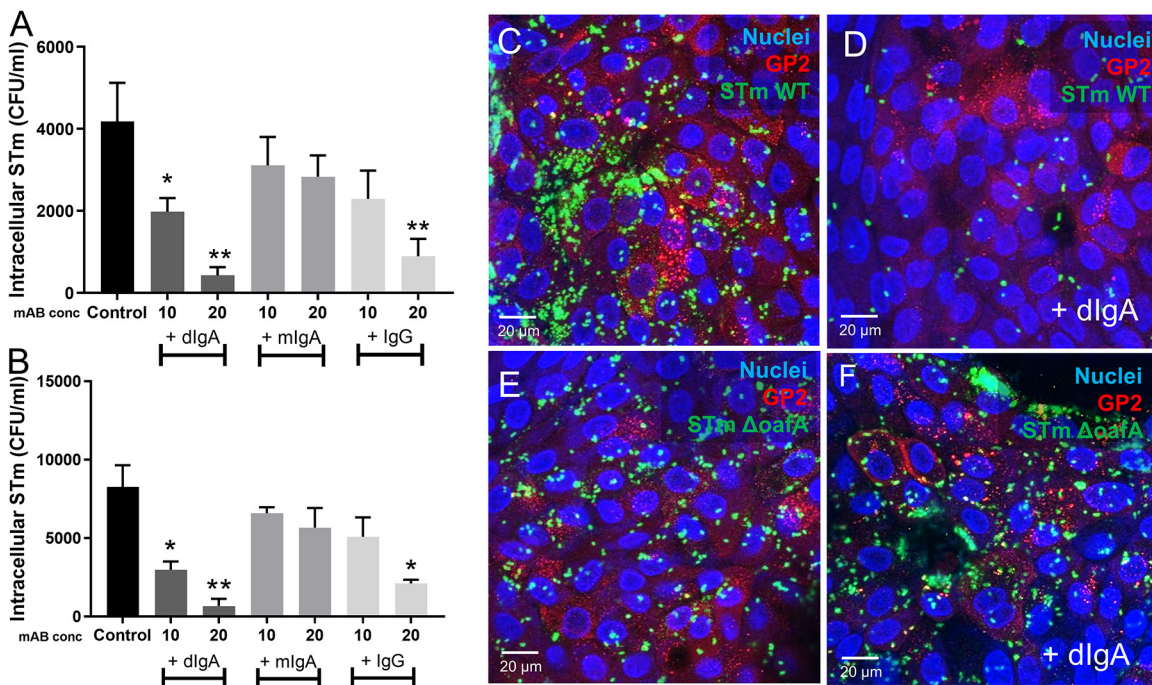
FIG 7 Basolateral addition of Sal4 IgA and Sal4 IgG reduces STm invasion Antibodies (10 or 20 μg/mL Sal4 dIgA, Sal4 mIgA and Sal4 IgG) were added to monolayers basolaterally for 16 h. Monolayers of Enteroids and HIOs were infected for 2 h with WT STm (0.01 OD_{600}). STm invasion was measured with a gentamicin invasion assay. In Enteroids (A) and HIOs (B), results show Sal4 dIgA and Sal4 IgG significantly reduced invasion of WT STm in a dose dependent manner, but not Sal4 mIgA. Monolayers of HIOs were incubated with no antibody or basolateral dSal4 for 16 h, and then infected with either WT or KO oafA STm for 2 h and costained for GP2 (red) and nuclei (blue). Confocal images show GFP WT STm co-stains with M cells (C) but not after addition of dSal4 (D). GFP KO oafA STm co-stains with M cells (E) and dIgA does not affect KO oafA co-staining with M cells (F). Images shown are representative images from ($n = 3$) technical replicates from ($n = 2$) biological experimental replicates. Bar graphs depict combined data from biological replicates ($n = 3$) $P < 0.05$, one-way ANOVA with Tukey post test.

monolayers were then challenged with STm, and bacterial invasion was quantified 2 h later through gentamicin protection assays (Fig. 7A and B). Interestingly, dIgA treatment significantly reduced STm invasion into both Enteroid and HIO monolayers, while mIgA did not. Specifically, STm invasion was reduced by ~20-fold in Enteroid and ~17-fold in HIOs when dSal4 (20 μg/mL) was applied basolaterally. In both Enteroid and HIOs, Sal4 IgG (20 μg/mL) also partially protected against invasion by STm (~5-fold in Enteroids and HIOs). The lower concentration (10 μg/mL) was only protective in HIOs, which could be linked to the higher levels of FCGRT. Finally, dSal4 reduced invasion into M-like cells, as demonstrated by confocal microscopy with GFP-tagged STm WT and co-staining for GP-2 (Fig. 7C–F). STm WT costained with GP2 antibody in the absence of dIgA, but not when dIgA is added basolaterally. Conversely, STm $\Delta oafA$ Sal4 which lacks the Sal4 epitope, costains with GP2 in the presence and absence of dSal4 (Fig. 7E–F).

DISCUSSION

Understanding the interplay between bacterial pathogens and the human intestinal epithelium is not complete without considering the mucosal immune system, a complex network of local gut-associated lymphoid tissues (e.g., Peyer's patches), antigen-presenting cells, T cell subsets and antibody-secreting B cells. Indeed, a cardinal feature of the human immune response to enteric pathogens like STm is the production of vast quantities of SIgA. While SIgA both shapes the gut microbiota and protects the epithelium from enteric pathogens, how SIgA accomplishes these two opposing tasks (e.g., promoting and preventing intestinal colonization) remains unknown. In this study, we demonstrated that the apical or basolateral addition of Sal4 MAbs were sufficient to protect both Enteroid and HIO-derived monolayers from STm infection. When added basolaterally, dIgA (but not mIgA) was transported across Enteroid and HIO-

derived monolayers into the apical Transwells compartment at sufficient levels to limit bacterial uptake. To our knowledge, this is the first demonstration of active dIgA transcytosis in an Enteroid or HIO model.

We confirmed that treatment of semiconfluent monolayers of Enteroids and HIOs with RANKL results in an increase in the formation of M-like cells (39, 40, 42, 43). We refer to them as "M-like cells" rather than *bona fide* M cells, which are characterized by a basolateral pocket occupied by leukocytes. In our hands, HIOs expressed more M-like cells than Enteroids in response to the same dose of RANKL. Whether this is due to the fact that our Enteroids are duodenal-derived, which is where Peyer's patches are concentrated, or other factors will be the subject of future studies (44). Nonetheless, the presence of increased numbers of M-like cells enhanced T3SS-1 dependent STm invasion. One limitation of our study is that we did not determine whether M-like cells facilitated STm transport across the epithelium. In other words, does STm exploit M-like cells in the Enteroids and HIO monolayers as gateways to breach the epithelial barrier like what occurs *in vivo* (45)? Or do M-like cells simply serve as a replicative niche? In the case of *Yersinia pseudotuberculosis* (*Yptb*) the presence of M-like cells in Enteroids resulted in increased bacterial uptake as well as transcytosis (46). *Yptb* also induced M-like cell extrusion from the monolayers, revealing another dimension of the host-pathogen interaction that can be modeled using organoids. Whether this occurs in the case of STm infection of Enteroids and HIOs remains to be determined.

In this study, we were able to recapitulate dIgA transcysosis from the basolateral to apical direction across Enteroid/HIO monolayers and detect the presence of SIgA in apical compartments. As noted earlier, secretion of IgA into the intestinal lumen requires pIgR, which transports polymeric IgA (or IgM) from the basolateral surface to the apical side. At the apical membrane, a portion of pIgR (secretory component) is cleaved by a host serine proteinase and remains bound to IgA, forming SIgA (11). pIgR can be overexpressed in intestinal cells by a variety of pro-inflammatory cytokines (47–49) however we chose IL-1 to induce pIgR to minimize damage to the intestinal monolayers. In Enteroid monolayers we showed that pIgR can be expressed at high levels and this enables transcytosis of IgA from the basolateral to the apical membrane as seen *in vivo*, and that the transcytosis results in formation of SIgA. *In vivo*, unbound pIgR can also be transcytosed via the endosome to the luminal side of the epithelium alongside with SIgA. It similarly undergoes cleavage and is released into the gut lumen as nonspecific targeting secretory component, which enhances adaptive immunity by protecting IgA from host degradation and proteases (50). In future studies it will be important to determine if this phenomenon is replicated in human organoid models. Studies have shown that secretory component can anchor IgA into in the intestinal mucus, with a likely 2-fold effect of agglutinating bacteria to be cleared in mucus secretions (50). In future work the Enteroid model could be used to study this phenomenon in further detail, particularly in a microfluidic device that could simulate the peristaltic and dynamic fluid flow of the intestine (51–54). We showed that HIOs expressed low levels of pIgR even with IL-1 stimulation, and much lower IgA transcytosis. Serum IgA levels are usually undetectable at birth in newborns, increasing throughout life and peaking in adolescence (55, 56). The lack of pIgR found in HIOs could be attributed to their fetal-like phenotype (21, 57), and as such they could be a useful tool to study the phenotypic switching events that occur in infant development, perhaps in conjunction with B-cell cocultures or other protocols that now exist for the maturation of HIOs which could potentially also improve pIgR expression, including bacterial stimulation, IL-2 and *in vivo* implantation (21, 36).

Our results with IgG reflect previous *in vivo* data where Sal4 IgG orally administered to mice was less effective than Sal4 IgA at protecting against Stm invasion (CITE). Interestingly, we also show here for the first time that Enteroids and HIOs express FCGRT. Originally identified in neonatal rats, it is now known that FCGRT is present in both fetal and adult tissues (58). While we saw almost no pIgR expression in HIOs, we found that FCGRT was upregulated, which also mimics what is seen in human fetus and newborns, where IgG/IgM are the primary host defense (56). Similarly, Navis (59)

found that mouse fetal organoids express high levels of FCGRT. Unlike pIgR, FCGRT is found on both apical and basolateral membranes and enables maternal IgG to protect against allergic reaction in the fetus through FCGRT mediated antigen presentation to dendritic cells, as well as allowing for bidirectional transport of immune complexes for antigen delivery to the lamina propria (60) in both fetus and adults. In a coculture model with intestinal myeloid cells, the Enteroid and HIO monolayers could be a useful tool to study signaling pathways involved in both human adult and fetal IgG transport and changes that occur in expression from immature (fetal) to mature (adult) tissue.

In this work, we have shown the potential for the Enteroid and HIO model to be used to identify critical pathways in this immune response due to the ability to mimic the immune-complex and mucosal membrane environment. Additionally, in future studies, we can use this model to elucidate any SIgA-M cell interactions. It should be noted that Enteroid and HIOs models have their shortcomings, especially when considering antibody functionality. Namely, they lack the myriad of physiological conditions in the gut that could affect the IgA and IgG localization, half-life and overall intestinal dynamics. For example, the mucus layer in Enteroid/HIOs is not necessarily representative of the thickness of the inner and outer mucus layers along the length of the GI tract (61). Enteroid/HIOs lack a microflora which would normally compete with STm for access to nutrients and even physical space along the epithelial surface (62, 63). Moreover, epithelial physiology is intrinsically different due to the fact that culture in an aerobic environment instead of the mostly anaerobic conditions of the intestinal lumen (64). Ultimately, more work is needed to develop an organoid-based GALT like Peyer's patch tissues with bonafide M cells with basolateral pockets populated by leukocytes (38, 65–68). Nevertheless, our data demonstrate the utility of Enteroid and HIO monolayer models for examining mucosal immunity in simplified models and provides the foundation for further studies of local antibody-mediated immunity.

MATERIALS AND METHODS

Intestinal tissue culture. HIOs were cultured from human induced pluripotent stem cells (hIPSCs) as described (69), with some modifications. Bone-marrow derived hIPSC line IISH1i-BM1 (Wicell) was expanded and maintained in mTesr (Stem Cell Technologies [SCT]). The hIPSCs were differentiated into endoderm using Definitive Endoderm kit (SCT). Hindgut was formed by adding 500 ng/mL FGF-4 (R&D systems) and 3 μM Chiron 99021 (Cayman) in RPMI with 2% FBS for 5 days until floating spheroids were formed. Floating hindgut spheroids were collected and embedded in Matrigel (BD Biosciences) with Intesticult (SCT) supplemented with 10 μM Rock Inhibitor (Cayman) 3 μM Chiron 99021. HIOs were passaged once a week for 6 weeks before experiments. Human Duodenal Enteroids were from the Baylor College of Medicine GEMs Core (22), received at passage 9 and maintained in Intesticult (SCT) in Matrigel beads.

HIO and enteroid monolayer formation. Transwells (24-well, Corning) were coated with 40 μg/mL human collagen (Sigma) in 0.6% acetic acid. HIOs and Enteroids were dissociated into single cells by adding TrypLE supplemented with 10 μM Rock Inhibitor for 20 min at 37°C. Cells were passed through a 40 μm cell strainer and resuspended in Intesticult with 10 μM Rock Inhibitor and 3 μM Chiron 99021. The cell concentration was adjusted to 1×10^6 cells/mL and 250 μL was seeded to the apical compartment of Transwells, with 500 μL Intesticult media added to the basolateral compartment. After 2 days, medium was changed to differentiation media (Advanced Dmem F12, 1$\times$ Glutamax, 1$\times$ B-27 supplement, 1 mM N-acetylcysteine, 500 nM A-8301, 100 ng/mL EGF, 100n ng/mL Noggin, 10 mM HEPES) and monolayers were cultured for a further 5 days. RANKL (Biolegend) 200 ng/mL was included in differentiation media for experiments with M-like cell formation. Monolayer integrity was verified by Lucifer Yellow exclusion before experiments.

siRNA knockdown of pIgR in enteroid and HIO monolayers. siRNA knockdown of pIgR was performed once monolayers reached ~70% confluence. Silencer Select siRNA for pIgR (1 μM working stock) and Lipofectamine RNAimax (3 μL per well) were mixed with Opti-MEM and added to monolayers for 36 h. siRNA knockdown was verified by qPCR for pIgR mRNA (primers: 5'ATTGCACAGGAGAAGTCGG, 3'CCTTCCACACTATTCACCTCC) with normalization to GAPDH (primers: 5'ACATCGCTCAGACACCATG, 3' TGTAGTTGAGGTCAATGAAGGG) and reduced expression of pIgR was confirmed by immunofluorescence using anti-pIgR antibody (Thermo).

Bacterial strains and growth conditions. Derivatives of *Salmonella* Typhimurium 14028s (*Salmonella enterica subsp. enterica* [ex Kauffmann and Edwards] Le Minor and Popoff serovar Typhimurium) were used in this study and are described in Table S1. Bacteria were maintained in Luria-Bertani (LB) at 37°C with aeration, unless otherwise noted. LB medium was supplemented with carbenicillin (100 μg/mL), kanamycin (50 μg/mL), or gentamicin (10 μg/mL) when appropriate. Recombineering constructs were designed using Benchling's cloud-based software platform and were engineered with primers (Table S2) custom synthesized by Integrated DNA Technologies (Coralville, IA). Plasmids used in fluorescent reporter strain construction were obtained through Addgene.org and are listed in Table S3. A detailed methodology describing STm deletion mutant and fluorescent reporter strain construction is provided

in the supplementary methods. For all experiments, WT bacteria and mutants were grown overnight in LB broth, then cultured to midlog-phase 0.5 OD_{600} before diluting into cell culture media.

Sal4 monoclonal IgG and IgA. Sal4 monomeric ($mIgA_2$) and dimeric IgA2 ($dIgA_2$) used in this study were generated as described (5). Chimeric Sal4 IgG1 was kindly provided by MappBiopharmaceutical (San Diego, CA).

Invasion assays. Monolayers of Enteroids and HIOs were infected apically with 0.01 OD_{600} STm (10^6 CFU/mL) for 2 h, with or without co-administration of Sal4 antibodies (dIgA, mIgA or IgG). Concentrations of antibodies were 1 μg/mL for apical experiments and 10 or 20 μg/mL for basolateral experiments. STm invasion was assessed through a gentamicin protection assay as previously described (70, 71). Briefly, nonadhered bacteria were removed by washing with PBS, followed by incubation with 250 μL gentamicin (150 μg/mL in DMEM) for 1 h to kill the adhered extracellular bacteria. Dead bacteria were removed by washing in PBS. For colony counts, monolayers were incubated with 500 μL 0.1% Triton X-100 for 15 min to lyse the cells and release the intracellular (invaded) bacteria. Serial fold dilutions and plating were then employed to determine CFU/mL invasion.

Immunofluorescence. For fluorescent staining of Enteroid and HIO monolayers, cells were fixed in 4% formaldehyde overnight at 4°C. Next, an antigen retrieval step was performed by incubating in 10 mM sodium-citrate buffer in a vegetable steamer for 20 min. The monolayers were then blocked with normal donkey serum (10% in PBS with 0.1% Triton X-100) for 2 h at RT. Samples were incubated overnight at 4°C with primary antibodies: rabbit anti-GP2, rabbit anti-pIgR, or rabbit anti-FCGRT or normal Rabbit IgG control (all from Thermo). All primary antibodies were used at 1:50 dilution in primary antibody buffer (1× PBS/1% BSA/0.1% Triton). Samples were then immersed in Alexa Flour 488 or 555 donkey anti-rabbit secondary antibodies (Thermo) at a 1:500 dilution in PBS-0.05% Tween 20 for 2 h at RT. Nuclei were stained with To-Pro-3 (1:1000 in PBS) for 30 min at RT. The monolayers were imaged using a Zeiss LSM880 Confocal/Multiphoton Upright Microscope, with 3-D image rendering using ImageJ.

RNA extraction and quantitative RT-PCR. HIOs and Enteroids monolayers were washed with PBS and RNA was isolated using a RNeasy minikit (Qiagen, MD). On column DNase (Qiagen) was used to remove any contaminating DNA and RNA purity and concentration was determined using a Nanodrop (Thermo). Reverse transcription of the RNA was performed using iScript cDNA Synthesis kit (Bio-Rad). A negative control with no reverse transcriptase was used in each data set. Primers are shown in table S4. Quantitative real-time PCR was performed with SsoAdvanced Universal SYBR green kit (Bio-Rad) with normalization to GAPDH and GUSB.

ELISA. STm LPS ELISAs were conducted as described by Richards (5). Clear Flat-Bottom Immuno 96-well plates (Thermo) were coated with 0.1 mL of STm LPS (1 μg/mL in sterile PBS) overnight at 4 ³C. Wells were blocked with PBS containing 0.1% Tween 20 (PBST) and 2% goat serum for 2 h before washing with PBST. Plates were developed using goat anti-human HRP-conjugated secondary IgG antibodies (final concentration of 0.5 μg/mL) and SureBlue TMB Microwell Peroxidase Substrate (KPL). A secretory IgA ELISA (Eagle biosciences) was used for measuring sIgA translocation to apical membrane according to manufacturer's instructions.

SUPPLEMENTAL MATERIAL

Supplemental material is available online only.

SUPPLEMENTAL FILE 1, XLSX file, 0.01 MB.

SUPPLEMENTAL FILE 2, PDF file, 0.2 MB.

REFERENCES

1. Van Puyvelde S, Pickard D, Vandelannoote K, Heinz E, Barbé B, de Block T, Clare S, Coomber EL, Harcourt K, Sridhar S, Lees EA, Wheeler NE, Klemm EJ, Mbuyi Kalonji L, Phoba MF, Falay D, Ngbonda D, Lunguya O, Jacobs J, Dougan G, Deborggraeve S. 2019. An African Salmonella typhimurium ST313 sublineage with extensive drug-resistance and signatures of host adaptation. Nat Commun 10(1):4280.

2. Martinoli C, Chiavelli A, Rescigno M. 2007. Entry route of Salmonella typhimurium directs the type of induced immune response. Immunity 27:975–984. https://doi.org/10.1016/j.immuni.2007.10.011.

3. Carter PB, Collins FM. 1974. The route of enteric infection in normal mice. J Experimental Medicine 39(5):1189–1203.

4. Jones BD, Ghori N, Falkow S. 1994. Salmonella-Typhimurium initiates murine infection by penetrating and destroying the specialized epithelial M-cells of the Peyers-patches. J Exp Med 180:15–23. https://doi.org/10.1084/jem.180.1.15.

5. Richards AF, Baranova DE, Pizzuto MS, Jaconi S, Willsey GG, Torres-Velez FJ, Doering JE, Benigni F, Corti D, Mantis NJ. 2021. Recombinant human secretory IgA induces Salmonella Typhimurium agglutination and limits

bacterial invasion into gut-associated lymphoid tissues. ACS Infect Dis 7: 1221–1235. https://doi.org/10.1021/acsinfecdis.0c00842.

6. Richards AF, Doering JE, Lozito SA, Varrone JJ, Willsey GG, Pauly M, Whaley K, Zeitlin L, Mantis NJ. 2020. Inhibition of invasive salmonella by orally administered IgA and IgG monoclonal antibodies. PLoS Negl Trop Dis 14(3):e0007803.

7. McCarthy N, Kraiczy J, Shivdasani RA. 2020. Cellular and molecular architecture of the intestinal stem cell niche. Nature Cell Biology 22(9):1033–1041.

8. Brandtzaeg P. 2013. Secretory IgA: designed for anti-microbial defense. Front Immunol 4:222. https://doi.org/10.3389/fimmu.2013.00222.

9. Kumar N, Arthur CP, Ciferri C, Matsumoto ML. 2020. Structure of the secretory immunoglobulin A core. Science 367(6481):1008–1014.

10. Stadtmueller BM, Huey-Tubman KE, López CJ, Yang Z, Hubbell WL, Bjorkman PJ. 2016. The structure and dynamics of secretory component and its interactions with polymeric immunoglobulins. Elife 4:5:e10640. https://doi.org/10.7554/eLife.10640.

11. Turula H, Wobus CE. 2018. The role of the polymeric immunoglobulin receptor and secretory immunoglobulins during mucosal infection and immunity. Viruses 10:237. https://doi.org/10.3390/v10050237.

12. Michetti P, Porta N, Mahan MJ, Slauch JM, Mekalanos JJ, Blum AL, Kraehenbuhl JP, Neutra MR. 1994. Monoclonal immunoglobulin A prevents adherence and invasion of polarized epithelial cell monolayers by Salmonella typhimurium. Gastroenterology 107(4):915–23.

13. Michetti P, Mahan MJ, Slauch JM, Mekalanos JJ, Neutra MR. 1992. Monoclonal secretory immunoglobulin A protects mice against oral challenge with the invasive pathogen Salmonella typhimurium. Infect Immun 60: 1786–1792. https://doi.org/10.1128/iai.60.5.1786-1792.1992.

14. Lim CH, Voedisch S, Wahl B, Rouf SF, Geffers R, Rhen M, Pabst O. 2014. Independent bottlenecks characterize colonization of systemic compartments and gut lymphoid tissue by salmonella. PLoS Pathog 10(7).

15. Forbes SJ, Eschmann M, Mantis NJ. 2008. Inhibition of Salmonella enterica serovar typhimurium motility and entry into epithelial cells by a protective antilipopolysaccharide monoclonal immunoglobulin A antibody. Infect Immun 76:4137–4144. https://doi.org/10.1128/IAI.00416-08.

16. Richards AF, Torres-Velez FJ, Mantis NJ. 2022. Salmonella uptake into gut-associated lymphoid tissues: implications for targeted mucosal vaccine design and delivery. Methods Mol Biol 2410:305–324.

17. Nickerson KP, Llanos-Chea A, Ingano L, Serena G, Miranda-Ribera A, Perlman L, Lima R, Sztein MB, Fasano A, Senger S, Faherty CS. 2021. A versatile human intestinal organoid-derived epithelial monolayer model for the study of enteric pathogens. Microbiol Spectr 9(1):e0000321.

18. Lawrence AE, Abuaita BH, Berger RP, Hill DR, Huang S, Yadagiri VK, Bons B, Fields C, Wobus CE, Spence JR, Young VB, O'Riordan MX. 2021. Salmonella enterica Serovar Typhimurium SPI-1 and SPI-2 shape the global transcriptional landscape in a human intestinal organoid model system. mBio 12(3):e00399-21.

19. Abuaita BH, Lawrence AE, Berger RP, Hill DR, Huang S, Yadagiri VK, Bons B, Fields C, Wobus CE, Spence JR, Young VB, O'Riordan MX. 2021. Comparative transcriptional profiling of the early host response to infection by typhoidal and non-typhoidal Salmonella serovars in human intestinal organoids. PLoS Pathog 17(10):e1009987.

20. Ranganathan S, Smith EM, Foulke-Abel JD, Barry EM. 2020. Research in a time of enteroids and organoids: how the human gut model has transformed the study of enteric bacterial pathogens. Gut Microbes 12(1): 1795492.

21. Watson CL, Mahe MM, Múnera J, Howell JC, Sundaram N, Poling HM, Schweitzer JI, Vallance JE, Mayhew CN, Sun Y, Grabowski G, Finkbeiner SR, Spence JR, Shroyer NF, Wells JM, Helmrath MA. 2014. An in vivo model of human small intestine using pluripotent stem cells. Nat Med 20: 1310–1314. https://doi.org/10.1038/nm.3737.

22. Zou WY, Blutt SE, Crawford SE, Ettayebi K, Zeng X-L, Saxena K, Ramani S, Karandikar UC, Zachos NC, Estes MK. 2019. Human intestinal enteroids: new models to study gastrointestinal virus infections. Methods Mol Biol 1576:229–247.

23. Kasendra M, Tovaglieri A, Sontheimer-Phelps A, Jalili-Firoozinezhad S, Bein A, Chalkiadaki A, Scholl W, Zhang C, Rickner H, Richmond CA, Li H, Breault DT, Ingber DE. 2018. Development of a primary human small intestine-on-a-chip using biopsy-derived organoids. Sci Rep 8:2871–2871. https://doi.org/10.1038/s41598-018-21201-7.

24. Kasendra M, Luc R, Yin J, Manatakis DV, Kulkarni G, Lucchesi C, Sliz J, Apostolou A, Sunuwar L, Obrigewitch J, Jang K-J, Hamilton GA, Donowitz M, Karalis K. 2020. Duodenum Intestine-Chip for preclinical drug assessment in a human relevant model. Elife 9. https://doi.org/10.7554/eLife.50135.

25. Kayisoglu O, Weiss F, Niklas C, Pierotti I, Pompaiah M, Wallaschek N, Germer C-T, Wiegering A, Bartfeld S. 2021. Location-specific cell identity rather than exposure to GI microbiota defines many innate immune signalling cascades in the gut epithelium. Gut 70:687–697. https://doi.org/10.1136/gutjnl-2019-319919.

26. Forbester JL, Goulding D, Vallier L, Hannan N, Hale C, Pickard D, Mukhopadhyay S, Dougan G. 2015. Interaction of Salmonella enterica Serovar Typhimurium with intestinal organoids derived from human induced pluripotent stem cells. Infect Immun 83:2926–2934. https://doi.org/10.1128/IAI.00161-15.

27. Geiser P, Di Martino ML, Samperio Ventayol VL, Eriksson J, Sima E, Al-Saffar AK, Ahl D, Phillipson M, Webb DL, Sundbom M, Hellström PM, Sellin ME. 2021. Salmonella enterica Serovar Typhimurium exploits cycling through epithelial cells to colonize human and murine enteroids. mBio 12(1):e02684-20.

28. Crowley SM, Han X, Allaire JM, Stahl M, Rauch I, Knodler LA, Vallance BA. 2020. Intestinal restriction of Salmonella Typhimurium requires caspase-1 and caspase-11 epithelial intrinsic inflammasomes. PLoS Pathog 16(4): e1008498.

29. Puschhof J, Pleguezuelos-Manzano C, Martinez-Silgado A, Akkerman N, Saftien A, Boot C, de Waal A, Beumer J, Dutta D, Heo I, Clevers H. 2021. Intestinal organoid cocultures with microbes. Nat Protoc 16:4633–4649. https://doi.org/10.1038/s41596-021-00589-z.

30. Williamson IA, Arnold JW, Samsa LA, Gaynor L, DiSalvo M, Cocchiaro JL, Carroll I, Azcarate-Peril MA, Rawls JF, Allbritton NL, Magness ST. 2018. A high-throughput organoid microinjection platform to study gastrointestinal microbiota and luminal physiology. Cellular and Molecular Gastroenterology and Hepatology 6(3):301–319.

31. Roh TT, Chen Y, Paul HT, Guo C, Kaplan DL. 2019. 3D bioengineered tissue model of the large intestine to study inflammatory bowel disease. Biomaterials 225:119517. https://doi.org/10.1016/j.biomaterials.2019.119517.

32. Braverman J, Yilmaz ÖH. 2018. From 3D organoids back to 2D enteroids. Dev Cell 44:533–534. https://doi.org/10.1016/j.devcel.2018.02.016.

33. Wang Y, Kim R, Gunasekara DB, Reed MI, DiSalvo M, Nguyen DL, Bultman SJ, Sims CE, Magness ST, Allbritton NL. 2017. Formation of human colonic crypt array by application of chemical gradients across a shaped epithelial monolayer. Cellular and Molecular Gastroenterology and Hepatology 5(2):113–130.

34. Nigro G, Hanson M, Fevre C, Lecuit M, Sansonetti PJ. 2019. Intestinal organoids as a novel tool to study microbes-epithelium interactions. Methods Mol Biol 1576:183–194.

35. Workman MJ, Gleeson JP, Troisi EJ, Estrada HQ, Kerns SJ, Hinojosa CD, Hamilton GA, Targan SR, Svendsen CN, Barrett RJ. 2018. Enhanced utilization of induced pluripotent stem cell–derived human intestinal organoids using microengineered chips. Cell Mol Gastroenterol Hepatol 5:669–677.e2. https://doi.org/10.1016/j.jcmgh.2017.12.008.

36. Jung KB, Lee H, Son YS, Lee M-O, Kim Y-D, Oh SJ, Kwon O, Cho S, Cho H-S, Kim D-S, Oh J-H, Zilbauer M, Min J-K, Jung C-R, Kim J, Son M-Y. 2018. Interleukin-2 induces the in vitro maturation of human pluripotent stem cell-derived intestinal organoids. Nat Commun 9:3039–3039. https://doi.org/10.1038/s41467-018-05450-8.

37. Yoshida S, Miwa H, Kawachi T, Kume S, Takahashi K. 2020. Generation of intestinal organoids derived from human pluripotent stem cells for drug testing. Sci Rep 10(1):5989.

38. Rouch JD, Scott A, Lei NY, Solorzano-Vargas RS, Wang J, Hanson EM, Kobayashi M, Lewis M, Stelzner MG, Dunn JC, Eckmann L, Martín MG. 2016. Development of functional microfold (M) cells from intestinal stem cells in primary human enteroids. PLoS One 28;11(1):e0148216.

39. de Lau W, Kujala P, Schneeberger K, Middendorp S, Li VS, Barker N, Martens A, Hofhuis S, DeKoter RP, Peters PJ, Nieuwenhuis E, Clevers H. 2012. Peyer's patch M cells derived from Lgr5(+) stem cells require SpiB and are induced by RankL in cultured "miniguts". Mol Cell Biol 32(18): 3639–47.

40. Knoop KA, Kumar N, Butler BR, Sakthivel SK, Taylor RT, Nochi T, Akiba H, Yagita H, Kiyono H, Williams IR. 2009. RANKL is necessary and sufficient to initiate development of antigen-sampling M cells in the intestinal epithelium. J Immunology 183(9):5738–47.

41. Pyzik M, Sand KMK, Hubbard JJ, Andersen JT, Sandlie I, Blumberg RS. 2019. The Neonatal Fc Receptor (FcRn): a Misnomer? Front Immunol 10: 1540.

42. Wood MB, Rios D, Williams IR. 2016. TNF-α augments RANKL-dependent intestinal M cell differentiation in enteroid cultures. American J Physiology Cell Physiology 311(3):C498–507.

43. Fasciano AC, Dasanayake GS, Estes MK, Zachos NC, Breault DT, Isberg RR, Tan S, Mecsas J. 2021. Yersinia pseudotuberculosis YopE prevents uptake

by M cells and instigates M cell extrusion in human ileal enteroid-derived monolayers. Gut Microbes 13(1):1988390.

44. Cornes JS. 1965. Number, size, and distribution of Peyer's patches in the human small intestine: part I The development of Peyer's patches. Gut 6(3):225–9.

45. Jones BD, Ghori N, Falkow S. 1994. Salmonella typhimurium initiates murine infection by penetrating and destroying the specialized epithelial M cells of the Peyer's patches. The J Experimental Medicine 180(1):15–23.

46. Fasciano AC, Blutt SE, Estes MK, Mecsas J. 2019. Induced differentiation of M cell-like cells in human stem cell-derived ileal enteroid monolayers. J Vis Exp 26:(149). https://doi.org/10.3791/59894.

47. Moon C, VanDussen KL, Miyoshi H, Stappenbeck TS. 2014. Development of a primary mouse intestinal epithelial cell monolayer culture system to evaluate factors that modulate IgA transcytosis. Mucosal Immunol 7:818–828. https://doi.org/10.1038/mi.2013.98.

48. Diebel LN, Liberati DM. 2011. Disparate effects of bacteria and toll-like receptor-dependant bacterial ligand stimulation on immunoglobulin A transcytosis. J Trauma 70:691–700. https://doi.org/10.1097/TA.0b013e31820c780e.

49. Bruno ME, Frantz AL, Rogier EW, Johansen FE, Kaetzel CS. 2011. Regulation of the polymeric immunoglobulin receptor by the classical and alternative NF-κB pathways in intestinal epithelial cells. Mucosal Immunology 4(4):468–78.

50. Rogier EW, Frantz AL, Bruno ME, Kaetzel CS. 2014. Secretory IgA is concentrated in the outer layer of colonic mucus along with gut bacteria. Pathogens (Basel, Switzerland) 3(2):390–403.

51. Costello CM, Phillipsen MB, Hartmanis LM, Kwasnica MA, Chen V, Hackam D, Chang MW, Bentley WE, March JC. 2017. Microscale bioreactors for in situ characterization of GI epithelial cell physiology. Sci Rep 7:12515–12515. https://doi.org/10.1038/s41598-017-12984-2.

52. Richardson A, Schwerdtfeger LA, Eaton D, Mclean I, Henry CS, Tobet SA. 2020. A microfluidic organotypic device for culture of mammalian intestines: ex vivo. Anal Methods 12:297–303. https://doi.org/10.1039/C9AY02038A.

53. Chi M, Yi B, Oh S, Park D-J, Sung JH, Park S. 2015. A microfluidic cell culture device (μFCCD) to culture epithelial cells with physiological and morphological properties that mimic those of the human intestine. Biomed Microdevices 17:9966–9958. https://doi.org/10.1007/s10544-015-9966-5.

54. Kim HJ, Huh D, Hamilton G, Ingber DE. 2012. Human gut-on-a-chip inhabited by microbial flora that experiences intestinal peristalsis-like motions and flow. Lab Chip 12:2165. https://doi.org/10.1039/c2lc40074j.

55. Shen C, Xu H, Liu D, Veazey RS, Wang X. 2014. Development of serum antibodies during early infancy in rhesus macaques: implications for humoral immune responses to vaccination at birth. Vaccine 32(41):5337–5342.

56. Weemaes C, Klasen I, Göertz J, Beldhuis-Valkis M, Olafsson O, Haraldsson A. 2003. Development of immunoglobulin A in infancy and childhood. Scandinavian J Immunology 58(6):642–8.

57. Finkbeiner SR, Hill DR, Altheim CH, Dedhia PH, Taylor MJ, Tsai Y-H, Chin AM, Mahe MM, Watson CL, Freeman JJ, Nattiv R, Thomson M, Klein OD, Shroyer NF, Helmrath MA, Teitelbaum DH, Dempsey PJ, Spence JR. 2015. Transcriptome-wide analysis reveals hallmarks of human intestine development and

maturation in vitro and in vivo. Stem Cell Rep 4:1140–1155. https://doi.org/10.1016/j.stemcr.2015.04.010.

58. Mikulska JE. 2015. Analysis of response elements involved in the regulation of the human neonatal Fc receptor gene *(FCGRT)*. PLoS ONE 10(8):e0135141. https://doi.org/10.1371/journal.pone.0135141.

59. Navis M, Martins Garcia T, Renes IB, Vermeulen JL, Meisner S, Wildenberg ME, van den Brink GR, van Elburg RM, Muncan V. 2019. Mouse fetal intestinal organoids: new model to study epithelial maturation from suckling to weaning. EMBO Rep 20(2):e46221.

60. Castro-Dopico T, Clatworthy MR. 2019. IgG and Fcγ receptors in intestinal immunity and inflammation. Front Immunol 10:805.

61. Engevik AC. 2020. Using microfluidics to model mucus. Cellular and Molecular Gastroenterology and Hepatology 9(3):551–552.

62. Litvak Y, Mon KKZ, Nguyen H, Chanthavixay G, Liou M, Velazquez EM, Kutter L, Alcantara MA, Byndloss MX, Tiffany CR, Walker GT, Faber F, Zhu Y, Bronner DN, Byndloss AJ, Tsolis RM, Zhou H, Bäumler AJ. 2019. Commensal Enterobacteriaceae protect against Salmonella colonization through oxygen competition. Cell Host Microbe 25:128–139.e5. https://doi.org/10.1016/j.chom.2018.12.003.

63. Rivera-Chávez F, Bäumler AJ. 2015. The pyromaniac inside you: Salmonella metabolism in the host gut. Annu Rev of Microbiology 69:31–48.

64. Fattinger SA, Sellin ME, Hardt WD. 2021. Epithelial inflammasomes in the defense against Salmonella gut infection. Current Opinion in Microbiology 59:86–94.

65. de Lau W, Kujala P, Schneeberger K, Middendorp S, Li VS, Barker N, Martens A, Hofhuis F, DeKoter RP, Peters PJ, Nieuwenhuis E, Clevers H. 2012. Peyer's Patch M cells derived from Lgr5+ stem cells require SpiB and are induced by RankL in cultured "miniguts." Mol Cell Biol 32(18):3639–47.

66. Jung C, Hugot JP, Barreau F. 2010. Peyer's Patches: the Immune Sensors of the Intestine. Int J Inflammation 2010:823710.

67. Mörbe UM, Jørgensen PB, Fenton TM, von Burg N, Riis LB, Spencer J, Agace WW. 2021. Human gut-associated lymphoid tissues (GALT); diversity, structure, and function. Mucosal Immunology 14(4):793–802.

68. Ahmad T, Gogarty M, Walsh EG, Brayden DJ. 2017. A comparison of three Peyer's patch "M-like" cell culture models: particle uptake, bacterial interaction, and epithelial histology. European J Pharmaceutics and Biopharmaceutics: official J Arbeitsgemeinschaft Fur Pharmazeutische Verfahrenstechnik eV 119:426–436.

69. Spence JR, Mayhew CN, Rankin SA, Kuhar MF, Vallance JE, Tolle K, Hoskins EE, Kalinichenko VV, Wells SI, Zorn AM, Shroyer NF, Wells JM. 2011. Directed differentiation of human pluripotent stem cells into intestinal tissue in vitro. Nature 470:105–120. https://doi.org/10.1038/nature09691.

70. Steele-Mortimer O. 2008. Infection of epithelial cells with Salmonella enterica. Methods Mol Biol 431:201–211.

71. Gagnon M, Zihler Berner A, Chervet N, Chassard C, Lacroix C. 2013. Comparison of the Caco-2, HT-29 and the mucus-secreting HT29-MTX intestinal cell models to investigate Salmonella adhesion and invasion. J Microbiol Methods 94:274–279. https://doi.org/10.1016/j.mimet.2013.06.027.